
Anomaly Detection via Gumbel Noise Score Matching

Ahsan Mahmood¹

Junier Oliva¹

Martin Styner¹

¹Department of Computer Science , University of North Carolina at Chapel Hill

Abstract

We propose Gumbel Noise Score Matching (GNSM), a novel unsupervised method to detect anomalies in categorical data. GNSM accomplishes this by estimating the scores, i.e. the gradients of log likelihoods w.r.t. inputs, of continuously relaxed categorical distributions. We test our method on a suite of anomaly detection tabular datasets. GNSM achieves a consistently high performance across all experiments.

We further demonstrate the flexibility of GNSM by applying it to image data where the model is tasked to detect poor segmentation predictions. Images ranked anomalous by GNSM show clear segmentation failures, with the outputs of GNSM strongly correlating with segmentation metrics computed on ground-truth. We outline the score matching training objective utilized by GNSM and provide an open-source implementation of our work.

1 INTRODUCTION

Anomaly detection on tabular data remains an unsolved problem Pang et al. [2021b], Ruff et al. [2021], Aggarwal [2017]. Notably, there are few methods in this space that explicitly model categorical data types (Pang et al. [2021a]). For instance, none of the methods tested in the recent comprehensive benchmark performed by Han et al. [2022] make explicit use of categorical information. After transforming the categorical variables into one-hot and binary encodings, existing methods proceed to treat them as distinct continuous variables. Furthermore, there is a dearth of unsupervised deep learning anomaly detection methods that excel on tabular datasets. For example, the otherwise exhaustive benchmark of Han et al. [2022] reports only two unsupervised deep learning models (DSVDD Ruff et al. [2018] and DAGMM Zong et al. [2018]) in their analysis; with both

models being outperformed by shallow unsupervised methods. Some reconstruction-based autoencoder approaches have been proposed Hawkins et al. [2002] but they require optimization tricks such as adaptive sampling, pretraining, and ensembling to work effectively Chen et al. [2017a].

To fill this gap, we propose a novel unsupervised method to detect anomalies: Gumbel Noise Score Matching (GNSM). Our method estimates the scores of continuous relaxations of categorical variables. Note that each relaxed categorical will be represented by the probability vector of all outcomes pertaining to that feature. It follows that the score (gradients of log likelihood) of a relaxed category will be defined over all outcomes. Thus, our model is implicitly aware of the distribution of outcomes for each categorical feature. We postulate that modeling this information will help our model identify samples composed of rarely occurring categories i.e. anomalies.

Our main contributions are :

- Deriving an unsupervised training objective for learning the scores of categorical distributions
- Demonstrating the capability of score matching for anomaly detection on categorical types in both tabular and image datasets
- Providing a unified framework for modeling mixed data types via score matching

To illustrate the significance of our last contribution, consider the Census dataset in our experiments (Section 5). We were able to compute the scores for both the continuous features (using standard denoising score matching Vincent [2011]) and the categorical features (using GNSM). Further still, our model is not limited to tabular data. As demonstrated in Section 6.2, GNSM can effectively detect anomalies in images (segmentation masks). This flexibility, paired with our simple loss objective, illustrates the practical viability of our method.

2 BACKGROUND

Our work combines continuous relaxations for categorical data Jang et al. [2017], Maddison et al. [2017] into the denoising score matching objective Vincent [2011]. We will briefly expand on some of the background material to provide context.

2.1 SCORE MATCHING

Hyvärinen [2005] introduced score matching as a methodology to estimate the gradient of the log density with respect to the data (i.e. the score): $\nabla_x \log p(x)$. If we assume a noise distribution $q_\sigma(\tilde{x}|x)$ is available, it is possible to learn the scores for the perturbed data distribution $q_\sigma(\tilde{x}) \triangleq \int q_\sigma(\tilde{x}|x)p(x)dx$. Vincent [2011] proved that that minimizing the Denoising Score Matching (DSM) objective in Equation (1) will train the score estimator s_θ to satisfy $s_\theta(x) = \nabla_x \log q_\sigma(x)$.

$$J_{\text{DSM}}(\theta) = \mathbb{E}_{q_\sigma} [\|s_\theta(x) - \nabla_{\tilde{x}} \log q_\sigma(\tilde{x}|x)\|^2] \quad (1)$$

Song and Ermon [2019] introduced Noise Conditioned Score Networks (NCSN) and expanded the DSM objective in (1) to include multiple noise distributions of increasing noise levels.

$$J_{\text{NCSN}}(\theta) = \sum_{i=1}^L \mathbb{E}_{q_{\sigma_i}} [\|s_\theta(x, \sigma_i) - \nabla_{\tilde{x}} \log q_{\sigma_i}(\tilde{x}|x)\|^2] \quad (2)$$

The authors’ main insight was to use the same model for all noise levels. They parameterized the network to accept noise scales as conditioning information. NCSNs were successful in generating images and have been shown to have close ties to generative diffusion models Song and Ermon [2019].

2.2 CONNECTING SCORE MATCHING TO ANOMALY DETECTION

While Song and Ermon [2019] demonstrated the generative capabilities of NCSNs, Mahmood et al. [2021] outlined how these networks can be repurposed for outlier detection. Their methodology, Multiscale Score Matching Analysis (MSMA), incorporates noisy score estimators to separate in- and out-of-distribution (OOD) points. Recall that a score is the gradient of the likelihood. A typical point, residing in a space of high probability density will need to take a small gradient step in order to improve its likelihood. Conversely, a point further away from the typical region (an outlier) will need to take a comparatively larger gradient step towards the high density region. When we have multiple noisy score estimates, it is difficult to know a priori which noise scale

accurately represents the gradient of the outliers. However, Mahmood et al. [2021], showed that learning the typical space of score-norms for all noise levels is sufficient to identify anomalies.

Concretely, assume we have a score estimator that is trained on L noise levels and a set of inlier samples X_{IN} . Computing the inlier score estimates for all noise levels and taking the L2-norms across the input dimensions results in an L -dimensional feature vector for each input sample: $[\|s(X_{\text{IN}}, \sigma_1)\|_2^2, \dots, \|s(X_{\text{IN}}, \sigma_L)\|_2^2]$. The authors in Mahmood et al. [2021] argue that inliers tend to concentrate in this multiscale score-norm embedding space. It follows that one could train an auxiliary model (such as a clustering model or a density estimator) to learn this score-norm space of inliers. At test time, the output of the auxiliary model (e.g. likelihoods in the case of density estimators) is used as an anomaly score. Results in Mahmood et al. [2021] show MSMA to be effective at identifying OOD samples in image datasets (e.g. CIFAR-10 as inliers SVHN as OOD).

2.3 CONTINUOUS RELAXATION TO CATEGORICAL DATA

Note that gradients of log likelihoods are not defined for categorical inputs. In order to compute the score of categorical data, we propose to adopt a continuous relaxation for discrete random variables co-discovered by Jang et al. [2017], Maddison et al. [2017]. These relaxations build on the Gumbel-Max trick to sample from a categorical distribution Maddison et al. [2014]. The procedure (often referred to as the Gumbel-Softmax) works by adding Gumbel noise Gumbel [1954] to the (log) probabilities and then passing the resulting vector through a softmax to retrieve a sharpened probability distribution over the categorical outcomes. Of particular interest to us, this procedure incorporates a temperature parameter (λ in Equation (3)) to control the sharpening of the resulting probabilities. We argue that this temperature can also be interpreted as a noise parameter, by virtue of it increasing the entropy of the post-softmax probabilities. We will make use of this intuition when we combine continuous relaxations with denoising score matching in Section 3.1.

For our work, we will be utilizing the formulation of Maddison et al. [2017] i.e. Concrete random variables. In particular, we will be using ExpConcrete Distribution as it is defined in the log domain. This is mainly done for convenience and numerical stability. Given unnormalized probabilities $\alpha \in (0, \infty)^K$, Gumbel i.i.d samples G_k , and a smoothing factor $\lambda \in (0, \infty)$ we can construct a $Y \in \mathbb{R}^n$ such that $\exp(Y) \sim \text{Concrete}(\alpha, \lambda)$:

$$Y_k = \frac{\log \alpha_k + G_k}{\lambda} - \log \sum_{i=1}^K \exp \left\{ \frac{\log \alpha_i + G_i}{\lambda} \right\} \quad (3)$$

As $\lambda \rightarrow 0$, the computation approaches an argmax, while large values of λ will push the random variable towards a uniform distribution.

3 SCORE MATCHING WITH CATEGORICAL VARIABLES

In this section we will develop the ideas behind our loss objective.

We start by noting that the proof of the denoising objective by Vincent [2011] (Equation (1)) holds true for any q_σ , provided that $\log q_\sigma(\tilde{x}|x)$ is differentiable. Recall that q_σ plays the role of a noise distribution. While most denoising score matching models incorporate Gaussian perturbation Song and Ermon [2019], Song et al. [2021], Vincent [2011], we emphasize that *any* noise distribution may be used during training.

3.1 EXPCONCRETE(α, λ) AS A NOISE DISTRIBUTION

Following the reasoning above and the temperature parameter (λ) available in Equation 3, we posit that one can repurpose the Concrete distribution to add ‘noise’ to our continuous relaxations of the categorical variables. Increasing λ will allow us to corrupt the input x by scaling the logits and smoothing out the categorical probabilities.

For our objective, we can set the noise distribution as:

$$\log q_\sigma(\tilde{\mathbf{x}}|\mathbf{x}) = \log p_\lambda(\tilde{\mathbf{x}}; \alpha = \mathbf{x})$$

Here we set the location parameter to that of the unperturbed input (similar to how one would use a Gaussian kernel) with λ being a known hyperparameter. Note that $\mathbf{x} \in \{0, 1\}^K$ will be a one-hot encoding for K outcomes, which does not satisfy the requirement $\alpha \in (0, \infty)^K$. This can be circumvented by adding a small delta to the vectors to avoid zero values. While it is possible to transform \mathbf{x} to any positive unnormalized probabilities, we opted to use the one-hot encodings for simplicity i.e. $\alpha = \mathbf{x} + \delta$.

3.2 DENOISING OBJECTIVE

Equation (4) represents the score function the ExpConcrete distribution i.e. the gradient of the log-density with respect to the data:

$$\nabla_{\tilde{\mathbf{x}}_j} \log p_\lambda(\tilde{\mathbf{x}}; \mathbf{x}) = -\lambda + \lambda K \sigma(\log \mathbf{x} - \lambda \tilde{\mathbf{x}})_j \quad (4)$$

where $\sigma(\mathbf{z})_i = \frac{e^{z_i}}{\sum_{k=1}^K e^{z_k}}$ is the softmax function. The complete derivation is available in the Appendix.

We can now combine the ideas from Denoising Score Matching and Concrete random variables. Combining Equation (1) and (4), we obtain

$$\begin{aligned} J(\theta) &= \mathbb{E}_{q_\sigma} [\|s_\theta(x) - \nabla_{\tilde{x}} \log q(\tilde{x}|x)\|^2] \\ &= \mathbb{E}_{p_\lambda} [\|s_\theta(\tilde{\mathbf{x}}) - \nabla_{\tilde{\mathbf{x}}} \log p_\lambda(\tilde{\mathbf{x}}|\mathbf{x})\|^2] \\ &= \mathbb{E}_{p_\lambda} [\|s_\theta(\tilde{\mathbf{x}}) - \nabla_{\tilde{\mathbf{x}}} \log p_\lambda(\tilde{\mathbf{x}}; \alpha = \mathbf{x})\|^2] \\ &= \mathbb{E}_{p_\lambda} [\|s_\theta(\tilde{\mathbf{x}}) - (-\lambda + \lambda K \sigma(\log \mathbf{x} - \lambda \tilde{\mathbf{x}}))\|^2] \\ &= \mathbb{E}_{p_\lambda} [\|s_\theta(\tilde{\mathbf{x}}) - \lambda K \sigma(\log \mathbf{x} - \lambda \tilde{\mathbf{x}}) + \lambda\|^2] \\ &= \mathbb{E}_{p_\lambda} [\|s_\theta(\tilde{\mathbf{x}}) - \lambda K \sigma(\epsilon) + \lambda\|^2] \end{aligned}$$

Here $\epsilon = \log \mathbf{x} - \lambda \tilde{\mathbf{x}}$ and can be loosely interpreted as the "logit noise" as it is the difference between the original logit probabilities and the perturbed vector. This formulation is analogous to the simplification utilized by Song et al. [2021], Ho et al. [2020]. It allows us to train the model to estimate the noise directly as the other variables are known constants. Assume a network ϵ_θ , that takes the input $\tilde{\mathbf{x}}$. Following Equation (4), we can parameterize a score network as $s_\theta(\tilde{\mathbf{x}})_j = -\lambda + \lambda K \sigma(\epsilon_\theta(\tilde{\mathbf{x}}))_j$. We train the network ϵ_θ to estimate the noise values ϵ by the objective below.

$$J(\theta) = \mathbb{E}_{p_\lambda} [\lambda^2 K^2 \|(\sigma(\epsilon_\theta(\tilde{\mathbf{x}})) - \sigma(\epsilon))\|^2] \quad (5)$$

Following Song and Ermon [2019], we can modify our loss to train a Noise Conditioned Score Network with L noise levels i.e. $\lambda \in \{\lambda_i\}_{i=1}^L$:

$$J(\theta) = \sum_{i=0}^L \lambda_i^2 K_d^2 \mathbb{E}_{\mathbf{x}_d \sim p_{\text{data}}} \mathbb{E}_{\tilde{\mathbf{x}}_d \sim p_{\lambda_i}} [\|K(\sigma(\epsilon_\theta(\tilde{\mathbf{x}}_d, \lambda_i)) - \sigma(\epsilon))\|^2]$$

Note that our network is now additionally conditioned on the noise level λ . Finally, our loss objective can be extended to incorporate data with multiple categorical features. For D categories we have:

$$\sum_{d=0}^D \sum_{i=0}^L \lambda_i^2 K_d^2 \mathbb{E}_{\mathbf{x}_d \sim p_{\text{data}}} \mathbb{E}_{\tilde{\mathbf{x}}_d \sim p_{\lambda_i}} [\|(\sigma(\epsilon_\theta(\tilde{\mathbf{x}}_d, \lambda_i)) - \sigma(\epsilon))\|^2] \quad (6)$$

Here, K_d represents the number of outcomes per category, x_d represents the one-hot vector of length K_d , and $\tilde{\mathbf{x}}_d$ is the continuous, noisy representation of x_d obtained after a Concrete (Gumbel-Softmax) transform.

Thus, we have shown that a Concrete relaxation allows us to model the scores of categorical variables by acting as the noise distribution in the Denoising Score Matching objective. The network will output the scores of the logits

representing the categorical feature. Intuitively, these scores are gradients pointing in the direction of the category that maximizes the likelihood of the datapoint.

3.3 ANOMALY DETECTION

Once a network is trained with the denoising objective in Equation (6), we propose to construct an embedding space to identify anomalies. For a given point x , we compute the score estimates for all noise perturbation levels. The resulting vector represents the L -dimensional multiscale embedding space:

$$\eta(x) = \left(\|s_\theta(x, \lambda_1)\|_2^2, \dots, \|s_\theta(x, \lambda_L)\|_2^2 \right) \quad (7)$$

where $s_\theta(x, \lambda_i)$ is the noise conditioned score network estimating $\nabla_x \log p_{\lambda_i}(x)$. Following the mechanism laid out by Mahmood et al. [2021], we learn “areas of *concentration*” of the inlier data in the L -dimensional embedding space ($\eta(x)$, for $x \sim p$). Concretely, we train a GMM on $\eta(X_{\text{IN}})$, where X_{IN} represents the set of inliers. At inference time, we first use our score network to compute the embedding space $\eta(x)$ for the test samples and then compute the likelihoods of the embeddings via the trained GMM. The negative of this likelihood is then assumed as the anomaly score for the test samples.

4 RELATED WORKS

Unsupervised anomaly detection has been tackled by a myriad of methods Pang et al. [2021b], Ruff et al. [2021], with varying success Han et al. [2022]. For the purposes of this work, we primarily focus on unsupervised anomaly detection algorithms that have been successfully applied to tabular data. Every algorithm employs its own assumptions and principles about normality Aggarwal [2017]. These principles can be elucidated into three broad detection methodologies:

4.1 CLASSIFICATION-BASED

Here we are referring to one-class objectives, which do not need labeled samples. For example, One-Class Support Vector Machines (OC-SVMs) Chen et al. [2001] try to find the tightest hyperplane around the dataset, while Deep Support Vector Data Descriptors (DSVDD) Ruff et al. [2018] will compute the minimal hypersphere that encloses the data. Both methods assume that inliers will fall under the margins, and consequently use the distance to the margin boundaries as a score of outlieriness.

4.2 DISTANCE-BASED

The assumption here is that outliers will be far away from neighbourhoods of inliers. For example, k-Nearest Neighbours Peterson [2009] will use the distance to the k-th nearest inlier point as a score of anomaly. Isolation Forests Liu et al. [2008] implicitly use this assumption by computing the number of partitions required to isolate a point. Samples that are far away from their neighbours will thus be isolated with fewer partitions and be labeled as anomalies.

4.3 DENSITY-BASED

These models assume that anomalies are located in low-density regions in the input space. The principle objective is then to learn the density function representative of the typical (training) data. A trained model will be used to assign probabilities to test samples, with low probabilities signifying anomalies. Examples include Gaussian Mixture Models (GMMs) Reynolds et al. [2009] and their deep learning counter part, Deep Autoencoding Gaussian Mixture Models (DAGMM) Zong et al. [2018]. Both models estimate the parameters for a mixture of Gaussians, which are then used to assign likelihoods at inference time. ECOD Li et al. [2022] uses a different notion of density and estimates the cumulative distribution function (CDF) for each feature in the data. It then uses the tail probabilities from each learned CDF to designate samples as anomalous.

Furthermore, we acknowledge that there are many methods built for anomaly detection in images such as Schlegl et al. [2019], Bergmann et al. [2020] and Defard et al. [2021]. However, they have yet to be successfully applied to tabular data and it is uncertain how to extend them to categorical data types. Conversely, some methods have been built to address *only* categorical data types such as Akoglu et al. [2012] (compression-based) and Pang et al. [2016, 2021a] (frequency-based). Unfortunately, it is difficult to find open-source implementations of these models. It is also non-obvious how to extend them to mixed continuous/discrete features. Our method on the other hand, can handle mixed data types by using the appropriate score matching objective for continuous and categorical features.

5 EXPERIMENTS

We designed two experiments to evaluate our methodology: a benchmark on tabular data and a vision-based case study. The tabular benchmark will quantitatively assess the performance of GNSM compared to baselines. The case study will demonstrate a real world use case of detecting anomalous segmentation masks.

Dataset	# Samples	# Anomalies	# Features
Bank	36548	4640	53
Census	280717	18568	396 (+5 cont.)
Chess	28029	27	40
CMC	1444	29	25
Probe	60593	4166	67
Solar	1023	43	41
U2R	60593	228	40

Table 1: Statistics of public benchmark datasets. All datasets other than Census are categorical only.

5.1 TABULAR BENCHMARK

We created an experimental testbed with categorical anomaly detection datasets sourced from a publicly available curated repository¹. Note that for our method, we need to know the number of outcomes for each category, to appropriately compute the softmax over the dimensions. This prevents us from using preprocessed datasets such as those made available by Han et al. [2022]. It is also why we could not use all the datasets in the curated repository, as some had been pre-binarized.

We first split the datasets into inliers and outliers. Next, we divided the inliers into an 80/10/10 split for train, validation, and test respectively. The validation set is used for early stopping and the checkpoint with the best validation loss is used for inference. The test set is combined with the outliers and used for assessing performance. The categorical features were first converted to one-hot vectors and then passed through a log transform to retrieve logits. We used Standard normalization to normalize any continuous features (only relevant for Census). We compute results over five runs with different seeds.

We chose four methods to represent baseline performance in lieu of a comprehensive analysis with multiple methods. We were inspired to go this route due to the thorough results reported by ADBench Han et al. [2022]. As the authors describe, no one method outperforms the rest. We picked two representatives for shallow unsupervised methods: Isolation Forests and ECOD. We picked these as they consistently give good performance across different datasets and require little to no hyper parameter tuning. There are much fewer options for unsupervised deep learning methods that have been shown to work on tabular datasets. We chose two models that are popular in this field: DAGMM and DSVDD. Note that these were the only unsupervised deep learning models reported by Han et al. [2022]. For a fair comparison, we tried to keep the number of model parameters at the same order of magnitude as ours when possible. However, this would often lead to numerical instability for DAGMM. Thus we manually tuned the DAGMM hyperparameters for

the best and most stable performance for each dataset.

For our score network, we used a ResNet-like architecture inspired by Gorishniy et al. [2021]. We replaced BatchNorm layers with LayerNorm and set Dropout to zero. The dimensions of the Linear layers in each block were set to 1024. All activations were set to GELU (Hendrycks and Gimpel [2016]) except for the final layer, which was set to LeakyReLU. The number of residual blocks was set to 20. To condition the model on the noise scales, we added a noise embedding layer similar to those used in diffusion models Song et al. [2021]. We used the same architecture across all datasets.

Our noise parameter λ is a geometric sequence from $\lambda = 2$ to $\lambda = 20$. Early testing showed that the models gave numerical issues for values lower than 2. For the upper-limit (i.e. the largest noise scale) we chose 20 as it works well to smooth out the probabilities to uniform across all datasets. We set the number of noise scales (L) to 20. We compute the score norms on the inliers (train+val) according to Equation 7 and train a GMM on the resulting features. The negative likelihoods computed from the GMM are the final outputs of our method.

Extensive architectural details are available in the appendix. We also open sourced our code.²

5.2 SEGMENTATION CASE STUDY

The task here is to learn the distribution of ground truth image, segmentation pairs. At inference time, our model will score the outputs of a pretrained segmentation model. Our hypothesis is that our method will correctly detect failure cases i.e. poor segmentations should be ranked higher on the anomaly scale.

While there are many ways to qualitatively define a failure, we will be using popular segmentation metrics (with respect to ground truth masks) as a proxy for performance. We posit that a useful anomaly score should correlate meaningfully with the ground truth segmentation accuracies.

We compare the anomaly scores against three common segmentation metrics: the Dice similarity coefficient (Dice), the mean surface distance (MSD), and the 95-th percentile Hausdorff distance (95-HD). We chose Dice as it is a popular segmentation metric that measures the overlap between the predicted masks and the ground truth. However, as Dice scores may overestimate performance, it is recommended to additionally report distance based metrics Valentini et al. [2014], Taha and Hanbury [2015]. These metrics compute the distance between the surfaces of the predictions and ground truth masks.

We train a convolutional noise conditioned score network

¹<https://sites.google.com/site/gspangsite/sourcecode/categoricaldata>

²GitHub link will be provided upon acceptance

on the train-set of the Pascal-VOC segmentation dataset Everingham et al. [2010]. The input to our model is a pair of images and the one-hot segmentation masks. The model predicts the scores for the segmentation masks only. We chose to use paired data rather than segmentations alone as we want the model to learn whether a segmentation is appropriate for the image.

As our test subject, we retrieved a pretrained DeepLabV3 segmentation model Chen et al. [2017b] from the publicly available PyTorch implementation³. This model was trained on a subset of the COCO dataset Lin et al. [2014], using only the 20 categories that are present in the Pascal VOC dataset. We computed the segmentation outputs on the validation set of Pascal VOC. The aforementioned segmentation metrics were then calculated between the predictions and ground truth segmentation masks.

We compare the performance of our method to a convolutional DSVD. While there may exist specialized segmentation uncertainty estimators, we argue that an unsupervised model provides a more apt comparison. It is reasonable to postulate that both our model and DSVD could be improved by additionally incorporating segmentation-specific objectives into the training, but that remains outside the scope of this study.

For our score matching network, we adopted the NCSN++ model used by Song et al. [2021]. The only significant change was in the input/output layers as we are predicting scores over one-hot segmentation masks. For DSVD, we used the implementation of the original authors Ruff et al. [2018]. To keep a fair comparison, we modified the code to use a modern architecture as the backbone (specifically EfficientNetV2 Tan and Le [2021]) and kept the number of parameters similar to our model. Both models were trained to convergence and the best checkpoints (tested over a validation split of the train-set) were used for the analysis.

6 RESULTS

6.1 PERFORMANCE ON TABULAR BENCHMARK

We report the Average Precision error (AP) which can also be interpreted as the Area Under the Precision Recall curve (AUPR). Average precision computes the mean precision over all possible detection thresholds. We chose to highlight AP over AUROC as it is a more apt measure for detecting anomalies, where we often have unbalanced classes. Additionally, precision measures the positive predictive value of a classification i.e. the true positive rate. This is a particularly informative measure for anomaly detection algorithms where we are preferentially interested in the performance over one class (outliers) than the other (inliers). We would

also like to note that our anomaly ratios in the test set do not correspond with the true anomaly ratio in the original dataset. This is due to our data splitting scheme where our test set is effectively only 10% the size of inliers.

Table 2 shows that our approach performs better or on par with baselines. GNSM achieves significant performance improvements over baselines for Census, Probe and U2R, respectively achieving a 6.61%, 2.09%, and 11.18% improvement over the next best method.

Results for CMC and Bank are less straightforward to interpret as the differences in the models are not statistically significant, made apparent by the large overlap in the standard deviations. This is especially true for deep learning models which have to be optimized via gradient descent. On Solar, ECOD outperforms the rest by a significant margin. However, between deep learning models, GNSM performs notably better. Lastly, every model struggled with Chess, quite possibly due to the exceptionally small anomaly ratio. While Isolation Forests achieves the highest mean, it is uncertain whether the win is statistically significant. One could easily opt in favor of the other methods for this dataset as they achieve more consistent results. Again, between deep learning models, GNSM performs better.

Overall, we observed that the shallow models give more stable and consistent results, with ECOD having the smallest standard deviations on average. Additionally, we note that the reported tabular anomaly detection datasets prove difficult for all algorithms. As such, no one method definitively outperforms the rest; an outcome that coincides with previous findings of Han et al. [2022], Pang et al. [2021b], Ruff et al. [2021]. However, it is our belief that results in Table 2 highlight GNSM as a performant contender in the suite of available algorithms for practitioners looking to detect anomalies in unlabeled data domains.

6.2 DETECTING SEGMENTATION FAILURES

We computed the anomaly scores from both GNSM and DSVD and ranked the images from most to least anomalous. Next, we took the top $K = 50$ images (out of 1449) and computed the Pearson correlation coefficients between the ground truth segmentation metrics and the anomaly scores. We chose the worst ranked images for our analysis as we are interested in the efficacy of these scores for identifying segmentation failures as opposed to assessing the quality of successful segmentations.

Figure 1 shows the correlations between the ground truth segmentation metrics and the anomaly scores from GNSM and DSVD. Recall that Dice is a similarity metric while MSD and 95-HD are both distance-based metrics. Therefore, we initially hypothesized that a good anomaly score should correlate negatively with Dice and positively with the distances. Our results show that GNSM correlates strongly in

³https://pytorch.org/vision/stable/models/generated/torchvision.models.segmentation.deeplabv3_mobilenet_v3_large

Dataset	Ano Ratio	IForests	ECOD	DAGMM	DSVDD	GNSM (Ours)
Bank	0.56	63.24 ± 1.74	66.52 ± 0.57	57.62 ± 3.36	67.18 ± 6.94	65.58 ± 3.45
Census	0.40	40.64 ± 2.07	40.96 ± 0.15	32.90 ± 5.00	41.18 ± 3.44	47.79 ± 2.29
Chess	0.01	2.31 ± 1.36	1.43 ± 0.05	1.08 ± 0.44	1.47 ± 0.54	1.60 ± 0.68
CMC	0.17	22.72 ± 1.57	23.79 ± 1.75	24.99 ± 5.75	21.99 ± 6.15	25.87 ± 9.93
Probe	0.41	92.95 ± 2.28	95.39 ± 0.38	66.40 ± 9.43	89.16 ± 8.40	97.48 ± 0.62
Solar	0.30	67.99 ± 3.48	72.23 ± 0.91	50.84 ± 5.19	51.21 ± 3.94	63.34 ± 5.41
U2R	0.04	52.74 ± 12.88	67.84 ± 1.39	10.06 ± 6.47	71.17 ± 24.65	82.35 ± 5.45

Table 2: Average Precision across multiple datasets. Higher is better. Each experiment was repeated with 5 different seeds and we report the mean and standard deviations across seeds. IForest and ECOD represent shallow models, while DAGMM and DSVDD represent deep learning models. Ano ratio refers to the ratio of anomalies in the test set.

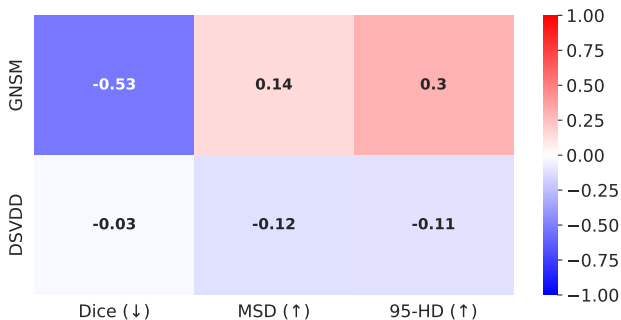


Figure 1: Correlations with segmentation metrics for Top- $K = 50$ anomaly scores retrieved from GNSM and Deep SVDD. The arrows next to the metric denote the expected correlation direction. The magnitude of the correlations reflects how well the anomaly scores capture segmentation errors.

the direction expected. DSVDD on the other hand achieved a poor correlation with Dice and inverse correlations with the distance based metrics. This signifies that our method is meaningfully capturing poor segmentations.

To qualitatively assess the results of each model and to explain the quantitative results, we visually inspected the worst ranked predictions alongside the groundtruth masks. A subset of the anomalous predictions are plotted in Figure 2. We observe that predictions ranked by GNSM in Figure 2a are either complete failures (most of the image is designated the background class) or severe under-segmentations. Predictions ranked by DSVDD in Figure 2b generally do not exhibit obvious segmentation failures, with most being reasonable predictions. Please look at the Appendix for all sorted $K = 50$ rankings.

7 LIMITATIONS

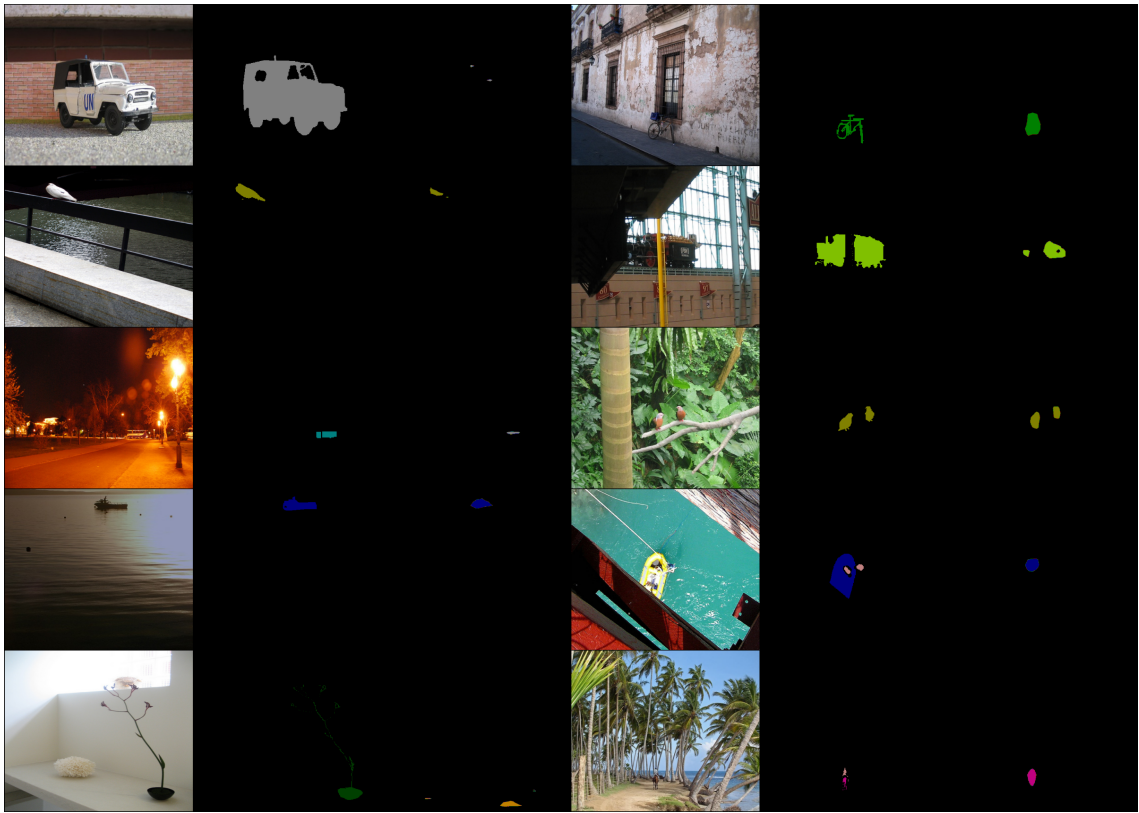
Early testing showed that our score networks need to be deep and require more parameters than baselines. Although our proposed network size is performant, we observed a trend of increased performance as the models got deeper

and wider. Due to time and resource constraints, we have not thoroughly explored the architecture space. Additionally, our model takes a significant number of iterations to converge. For our experiments, we trained for 1 million iterations, which can take up to a day of training. This is admittedly in contrast to the baselines which may take a few seconds for shallow models and up to a few hours for the deep learning models.

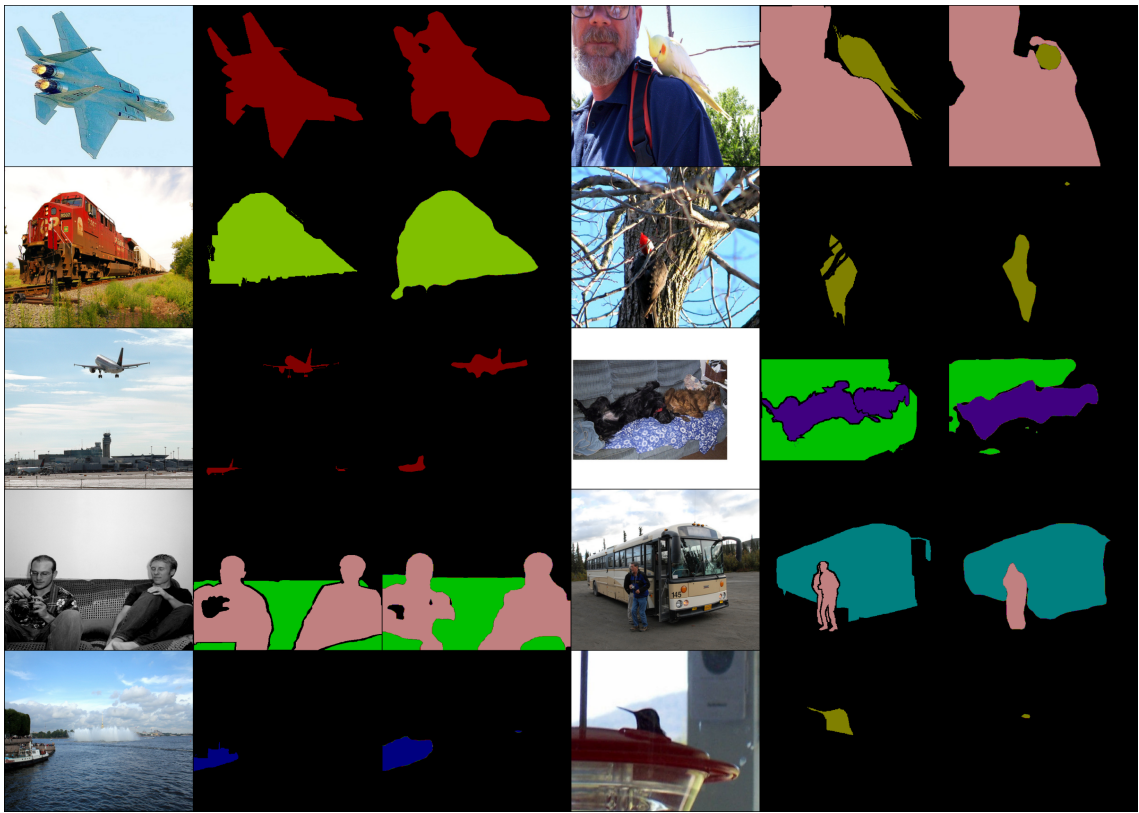
Furthermore, our model explicitly needs to know the number of outcomes per category to appropriately add noise and compute the scores. While we believe this to be a strength of our approach, it does make for an overhead on the user’s part. The baselines do not require this additional modeling complexity and are more straightforward to apply. Lastly, our method has hyperparameters pertaining to noise such as the number of scales used and the range of noise levels. While our hyperparameters have been proven to be stable, we posit that additional improvements may be obtained if these were also tuned per dataset.

8 CONCLUSION

In this work we introduced Gumbel Noise Score Matching (GNSM): a novel method for detecting anomalies in categorical data types. We outline how to compute scores of continuously relaxed categorical data and derive the appropriate training objective based on denoising score matching. Our method can easily be used in conjunction with standard score matching to model both continuous and categorical data. GNSM achieves competitive performance with respect to baselines on a suite of tabular anomaly detection datasets, attaining significant improvements on certain datasets. Furthermore, GNSM can easily be extended to images and excels on the real-world task of detecting anomalous segmentations. Lastly, we believe our novel categorical score matching formulation could be incorporated into generative models. We hope to explore this direction in future work.



(a) Random samples from Top-K=50 GNSM rankings. Note how the predicted segmentations are either partial/missing or include incorrect classes.



(b) Random samples from Top-K=50 DSVDD rankings. Note how only a few predictions may be considered anomalous.

Figure 2: Random samples from Top-K=50 anomaly rankings. The columns (repeated twice) show input image, ground truth segmentations, and model predictions respectively. Different classes are denoted by color.

References

- Charu C. Aggarwal. An Introduction to Outlier Analysis. In *Outlier Analysis*, pages 1–34. Springer International Publishing, Cham, 2017. ISBN 978-3-319-47578-3. doi: 10.1007/978-3-319-47578-3_1. URL https://doi.org/10.1007/978-3-319-47578-3_1.
- Leman Akoglu, Hanghang Tong, Jilles Vreeken, and Christos Faloutsos. Fast and reliable anomaly detection in categorical data. In *Proceedings of the 21st ACM International Conference on Information and Knowledge Management, CIKM '12*, page 415–424, New York, NY, USA, 2012. Association for Computing Machinery. ISBN 9781450311564. doi: 10.1145/2396761.2396816. URL <https://doi.org/10.1145/2396761.2396816>.
- Paul Bergmann, Michael Fauser, David Sattlegger, and Carsten Steger. Uninformed students: Student-teacher anomaly detection with discriminative latent embeddings. In *Proceedings of the IEEE/CVF Conference on Computer Vision and Pattern Recognition (CVPR)*, June 2020.
- Jinghui Chen, Saket Sathé, Charu Aggarwal, and Deepak Turaga. Outlier detection with autoencoder ensembles. In *Proceedings of the 2017 SIAM international conference on data mining*, pages 90–98. SIAM, 2017a.
- Liang-Chieh Chen, George Papandreou, Florian Schroff, and Hartwig Adam. Rethinking atrous convolution for semantic image segmentation. *arXiv preprint arXiv:1706.05587*, 2017b.
- Yunqiang Chen, Xiang Sean Zhou, and T.S. Huang. One-class svm for learning in image retrieval. In *Proceedings 2001 International Conference on Image Processing (Cat. No.01CH37205)*, volume 1, pages 34–37 vol.1, 2001. doi: 10.1109/ICIP.2001.958946.
- Thomas Defard, Aleksandr Setkov, Angelique Loesch, and Romaric Audigier. Padim: a patch distribution modeling framework for anomaly detection and localization. In *Pattern Recognition. ICPR International Workshops and Challenges: Virtual Event, January 10–15, 2021, Proceedings, Part IV*, pages 475–489. Springer, 2021.
- M. Everingham, L. Van Gool, C. K. I. Williams, J. Winn, and A. Zisserman. The pascal visual object classes (voc) challenge. *International Journal of Computer Vision*, 88(2):303–338, June 2010.
- Yury Gorishniy, Ivan Rubachev, Valentin Khruikov, and Artem Babenko. Revisiting deep learning models for tabular data. *Advances in Neural Information Processing Systems*, 34:18932–18943, 2021.
- Emil Julius Gumbel. *Statistical theory of extreme values and some practical applications: a series of lectures*, volume 33. US Government Printing Office, 1954.
- Songqiao Han, Xiyang Hu, Hailiang Huang, Minqi Jiang, and Yue Zhao. ADBench: Anomaly detection benchmark. In *Thirty-sixth Conference on Neural Information Processing Systems Datasets and Benchmarks Track*, 2022. URL https://openreview.net/forum?id=foA_SFQ9zo0.
- Simon Hawkins, Hongxing He, Graham Williams, and Rohan Baxter. Outlier detection using replicator neural networks. In *Data Warehousing and Knowledge Discovery: 4th International Conference, DaWaK 2002 Aix-en-Provence, France, September 4–6, 2002 Proceedings 4*, pages 170–180. Springer, 2002.
- Dan Hendrycks and Kevin Gimpel. Gaussian error linear units (gelus), 2016. URL <https://arxiv.org/abs/1606.08415>.
- Jonathan Ho, Ajay Jain, and Pieter Abbeel. Denoising diffusion probabilistic models. *Advances in Neural Information Processing Systems*, 33:6840–6851, 2020.
- Aapo Hyvärinen. Estimation of non-normalized statistical models by score matching. *Journal of Machine Learning Research*, 6(Apr):695–709, 2005.
- Eric Jang, Shixiang Gu, and Ben Poole. Categorical reparametrization with gumble-softmax. In *International Conference on Learning Representations (ICLR 2017)*. OpenReview.net, 2017.
- Zheng Li, Yue Zhao, Xiyang Hu, Nicola Botta, Cezar Ionescu, and George Chen. Ecod: Unsupervised outlier detection using empirical cumulative distribution functions. *IEEE Transactions on Knowledge and Data Engineering*, 2022. Publisher: IEEE.
- Tsung-Yi Lin, Michael Maire, Serge J. Belongie, Lubomir D. Bourdev, Ross B. Girshick, James Hays, Pietro Perona, Deva Ramanan, Piotr Dollár, and C. Lawrence Zitnick. Microsoft COCO: common objects in context. *CoRR*, abs/1405.0312, 2014. URL <http://arxiv.org/abs/1405.0312>.
- Fei Tony Liu, Kai Ming Ting, and Zhi-Hua Zhou. Isolation forest. In *2008 Eighth IEEE International Conference on Data Mining*, pages 413–422, 2008. doi: 10.1109/ICDM.2008.17.
- C Maddison, A Mnih, and Y Teh. The concrete distribution: A continuous relaxation of discrete random variables. In *Proceedings of the international conference on learning Representations*. International Conference on Learning Representations, 2017.
- Chris J Maddison, Daniel Tarlow, and Tom Minka. A* sampling. *Advances in neural information processing systems*, 27, 2014.

- Ahsan Mahmood, Junier Oliva, and Martin Andreas Styner. Multiscale score matching for out-of-distribution detection. In *International Conference on Learning Representations*, 2021. URL <https://openreview.net/forum?id=xoHdgbQJohv>.
- Guansong Pang, Longbing Cao, and Ling Chen. Outlier detection in complex categorical data by modelling the feature value couplings. In *Proceedings of the Twenty-Fifth International Joint Conference on Artificial Intelligence, IJCAI'16*, page 1902–1908. AAAI Press, 2016. ISBN 9781577357704.
- Guansong Pang, Longbing Cao, and Ling Chen. Homophily outlier detection in non-iid categorical data. *Data Mining and Knowledge Discovery*, 35:1163–1224, 2021a.
- Guansong Pang, Chunhua Shen, Longbing Cao, and Anton Van Den Hengel. Deep Learning for Anomaly Detection: A Review. *ACM Comput. Surv.*, 54(2), March 2021b. ISSN 0360-0300. doi: 10.1145/3439950. URL <https://doi.org/10.1145/3439950>. Place: New York, NY, USA Publisher: Association for Computing Machinery.
- Ethan Perez, Florian Strub, Harm De Vries, Vincent Dumoulin, and Aaron Courville. Film: Visual reasoning with a general conditioning layer. In *Proceedings of the AAAI Conference on Artificial Intelligence*, volume 32, 2018.
- Leif E Peterson. K-nearest neighbor. *Scholarpedia*, 4(2): 1883, 2009.
- Douglas A Reynolds et al. Gaussian mixture models. *Encyclopedia of biometrics*, 741(659-663), 2009.
- Lukas Ruff, Robert Vandermeulen, Nico Goernitz, Lucas Deecke, Shoaib Ahmed Siddiqui, Alexander Binder, Emmanuel Müller, and Marius Kloft. Deep one-class classification. In Jennifer Dy and Andreas Krause, editors, *Proceedings of the 35th International Conference on Machine Learning*, volume 80 of *Proceedings of Machine Learning Research*, pages 4393–4402. PMLR, 10–15 Jul 2018. URL <https://proceedings.mlr.press/v80/ruff18a.html>.
- Lukas Ruff, Jacob R. Kauffmann, Robert A. Vandermeulen, Grégoire Montavon, Wojciech Samek, Marius Kloft, Thomas G. Dietterich, and Klaus-Robert Müller. A Unifying Review of Deep and Shallow Anomaly Detection. *Proceedings of the IEEE*, 109(5):756–795, May 2021. ISSN 1558-2256. doi: 10.1109/JPROC.2021.3052449.
- Thomas Schlegl, Philipp Seeböck, Sebastian M Waldstein, Georg Langs, and Ursula Schmidt-Erfurth. f-anogan: Fast unsupervised anomaly detection with generative adversarial networks. *Medical image analysis*, 54:30–44, 2019.
- Yang Song and Stefano Ermon. Generative modeling by estimating gradients of the data distribution. *Advances in Neural Information Processing Systems*, 32, 2019.
- Yang Song, Jascha Sohl-Dickstein, Diederik P Kingma, Abhishek Kumar, Stefano Ermon, and Ben Poole. Score-based generative modeling through stochastic differential equations. In *International Conference on Learning Representations*, 2021. URL <https://openreview.net/forum?id=PxtTIG12RRHS>.
- Abdel Aziz Taha and Allan Hanbury. Metrics for evaluating 3d medical image segmentation: analysis, selection, and tool. *BMC medical imaging*, 15(1):1–28, 2015.
- Mingxing Tan and Quoc Le. Efficientnetv2: Smaller models and faster training. In *International conference on machine learning*, pages 10096–10106. PMLR, 2021.
- Vincenzo Valentini, Luca Boldrini, Andrea Damiani, and Ludvig P Muren. Recommendations on how to establish evidence from auto-segmentation software in radiotherapy. *Radiotherapy and Oncology*, 112(3):317–320, 2014.
- Pascal Vincent. A connection between score matching and denoising autoencoders. *Neural computation*, 23(7):1661–1674, 2011.
- Yue Zhao, Zain Nasrullah, and Zheng Li. Pyod: A python toolbox for scalable outlier detection. *Journal of Machine Learning Research*, 20(96):1–7, 2019. URL <http://jmlr.org/papers/v20/19-011.html>.
- Bo Zong, Qi Song, Martin Renqiang Min, Wei Cheng, Cristian Lumezanu, Daeki Cho, and Haifeng Chen. Deep autoencoding gaussian mixture model for unsupervised anomaly detection. In *International Conference on Learning Representations*, 2018. URL <https://openreview.net/forum?id=BJJLHbb0->.

A APPENDIX

A.1 SCORE OF EXPCONCRETE DISTRIBUTION

In this section, we compute the score for the ExpConcrete distribution i.e. take the gradient of the log-density with respect to the data. Conveniently, the authors of Maddison et al. [2017] derived the log-density of an ExpConcrete random variable, which we will be using going forward:

$$\log p_{\alpha, \lambda}(x) = \log((K-1)!) + (K-1) \log \lambda + \left(\sum_{k=1}^K \log \alpha_k - \lambda x_k \right) - K \log \sum_{k=1}^K e^{(\log \alpha_k - \lambda x_k)} \quad (8)$$

Here $x \in \mathbb{N}$ such that $\log \sum_{k=1}^K \exp(x) = 0$.

Since the first two terms in $\log p_{\alpha, \lambda}(x)$ (Equation (8)) are independent of x , we can ignore them and focus on the latter:

$$\nabla_{x_j} \log p_{\alpha, \lambda}(\mathbf{x}) = \nabla_{x_j} \left(\sum_{k=1}^K \log \alpha_k - \lambda x_k \right) - \nabla_{x_j} \left(K \log \sum_{k=1}^K \exp \{ \log \alpha_k - \lambda x_k \} \right) \quad (9)$$

$$= \nabla_{x_j} \left(- \sum_{k=1}^K \lambda x_k \right) - K \left(\nabla_{x_j} \log \sum_{k=1}^K \exp \{ \log \alpha_k - \lambda x_k \} \right) \quad (10)$$

$$= -\lambda - K \frac{\nabla_{x_j} \left(\sum_{k=1}^K \exp \{ \log \alpha_k - \lambda x_k \} \right)}{\sum_{k=1}^K \exp \{ \log \alpha_k - \lambda x_k \}} \quad (11)$$

$$= -\lambda - K \frac{\exp \{ \log \alpha_j - \lambda x_j \} \nabla_{x_j} (\log \alpha_j - \lambda x_j)}{\sum_{k=1}^K \exp \{ \log \alpha_k - \lambda x_k \}} \quad (12)$$

$$= -\lambda - K \frac{\exp \{ \log \alpha_j - \lambda x_j \} (-\lambda)}{\sum_{k=1}^K \exp \{ \log \alpha_k - \lambda x_k \}} \quad (13)$$

$$= -\lambda + \lambda K \frac{\exp \{ \log \alpha_j - \lambda x_j \}}{\sum_{k=1}^K \exp \{ \log \alpha_k - \lambda x_k \}} \quad (14)$$

Note how the last equation can be rewritten as:

$$\nabla_{x_j} \log p_{\alpha, \lambda}(\mathbf{x}) = -\lambda + \lambda K \sigma(\log \alpha - \lambda \mathbf{x})_j \quad (15)$$

where $\sigma(\mathbf{z})_i = \frac{e^{z_i}}{\sum_{k=1}^K e^{z_k}}$ is the softmax function.

A.2 EXPERIMENT DETAILS

A.2.1 Hyperparameters

ECOD is hyperparameter free so no tuning was required. Early testing showed that Isolation Forests hyperparameters were stable. Note that we did not use labelled anomalies during hyperparameter tuning and the rest of the deep learning models were tuned on an inlier-only validation set.

GNSM Networks

$$\sum_{d=0}^D \sum_{i=0}^L \lambda_i^2 K_d^2 \mathbb{E}_{\mathbf{x}_d \sim p_{\text{data}}} \mathbb{E}_{\tilde{\mathbf{x}}_d \sim p_{\lambda_i}} [\| (\sigma(\epsilon_\theta(\tilde{\mathbf{x}}_d, \lambda_i)) - \sigma(\epsilon)) \|^2] \quad (16)$$

Observing the loss in Equation 16, we see that we are minimizing the difference between two distributions as both inner terms pass through a softmax function. This insight led us to postulate that that we could substitute the mean squared error loss (MSE) for a metric more apt for matching distributions. We therefore ran experiments with KL divergence, which showed faster convergence than MSE. However this result is only empirical and we argue that tuning the optimization algorithm for MSE might gain similar improvements.

$$J(\theta) = \sum_{d=0}^D \sum_{i=0}^L \lambda_i^2 K_d^2 \mathbb{E}_{\mathbf{x} \sim p_{\text{data}}} \mathbb{E}_{\tilde{\mathbf{x}} \sim p_{\lambda_i}} [D_{\text{KL}}(\sigma(\epsilon) \parallel \sigma(\epsilon_{\theta}(\tilde{\mathbf{x}}_d))] \quad (17)$$

Most of these details are easily identifiable in our open source code. However, we still provide basic information for posterity. We used the same ResNet-like architecture for all datasets:

$$t = \text{TimeEmbeddingLayer}(\lambda) \quad (18)$$

$$\text{Net}(x, t) = \text{Head}(\text{ResBlock}(\dots \text{ResBlock}(x, t))) \quad (19)$$

$$\text{ResBlock}(x, t) = x + \text{Linear}(\text{FiLM}(x, t)) \quad (20)$$

$$\text{Head} = \text{Linear}(\text{LeakyReLU}(\text{LayerNorm}(x))) \quad (21)$$

Note that the FiLM block is taken from Perez et al. [2018] and the TimeEmbeddingLayer is the same as used in diffusion models Song et al. [2021], using the GaussianFourierProjection. A simplified implementation of the ResBlock is shown below.

```
class TabResBlockpp(nn.Module):
    def __init__(self, d_in, d_out, time_emb_sz, act="gelu", dropout=0.0):

        self.norm = nn.LayerNorm(d_in)
        self.dense_1 = nn.Linear(d_in, d_out)
        self.act = get_act(act)
        self.film = FiLMBlock(time_emb_sz, d_out)
        self.dropout = nn.Dropout(dropout)
        self.dense_2 = nn.Linear(d_out, d_out)

    def forward(self, x, t):

        h = self.act(self.norm(x))
        h = self.dense_1(h)
        h = self.film(h, t)
        h = self.dropout(h)
        h = self.dense_2(h)

    return x + h
```

For Bank we trained for 2MM iterations while for CMC and Solar, we trained for 600K iterations (as they were significantly smaller datasets). All the other models were trained for 1MM iters. We used the AdamW optimizer with default paramaters. The learning rate was set to $1e - 3$ with a cosine decay to $1e - 5$ spanning the number of iterations. We also use an Exponential Moving Average of the weights at a decay rate of 0.999. The base config is shown below.

```
def get_config():
    config = ml_collections.ConfigDict()
    # training
    config.training = training = ml_collections.ConfigDict()
    training.batch_size = 2048 # Except for CMC and Solar where it was 512
    training.n_steps = 1000001
    training.snapshot_freq = 10000 # Number of iterations for checkpointing

    # evaluation
```

```

config.eval = evaluate = ml_collections.ConfigDict()
evaluate.batch_size = 1024

# data config holds information about the dataset such as number of categories
config.data = data = ml_collections.ConfigDict()

# default model parameters
config.model = model = ml_collections.ConfigDict()
model.name = "tab-resnet"
model.tau_min = 2.0
model.tau_max = 20
### Only relevant for Census
model.sigma_min = 1e-1
model.sigma_max = 1.0
####
model.num_scales = 20
model.ndims = 1024
model.time_embedding_size = 128
model.layers = 20
model.dropout = 0.0
model.act = "gelu"
model.embedding_type = "fourier"
model.ema_rate = 0.999

# optimization
config.optim = optim = ml_collections.ConfigDict()
optim.weight_decay = 1e-4
optim.optimizer = "AdamW"
optim.lr = 1e-3
optim.beta1 = 0.9
optim.beta2 = 0.999
optim.grad_clip = 1.0
optim.scheduler = "cosine"

```

Lastly for MSMA, we train a GMM on the combined train, val set. We run a small grid search over number of components (3,5,7,9) and pick the one with best likelihood.

DSVDD

For Deep SVDD we used the implementation available in the PyOD library Zhao et al. [2019]. Initial testing showed that the autoencoder variant of this model usually performed better. This version adds a reconstruction loss to the one-class objective for increased regularization. The hidden neurons were set to [1024, 512, 256], with the `swish` activation function. Training was done with the Adam optimizer at default hyperparameters, with learning rate set to 1e-3. We trained for 1000 epochs, with the batch size set to 512.

DAGMM

DAGMM proved to be very difficult to train as most implementations often unexpectedly result in NaNs. In fact the implementation used by Han et al. [2022] never seemed to converge for any dataset. and the loss would not improve no matter how much we tweaked the hyperparameters. We believe the matrix inverse operation during the forward pass to be the culprit for this numerical instability.

We settled on modifying a publicly available PyTorch implementation⁴. We added the following changes to improve stability and performance:

- Added Layer Normalization

⁴<https://github.com/lixiangwang/DAGMM-pytorch>

- Added weight initialization
- Included checkpointing and early stopping using val set
- GMM parameters converted to double (float64)

Furthermore, we hand tuned hyperparameters for each dataset to find the most optimal (stable + performant) setting. Essentially, we tried to start from the same hyperparameters as DSVDD and tweaked until we got a stable model. We also early stopped on the checkpoint that gave the best validation loss (tested every epoch). If a NaN was encountered before the first epoch was finished (i.e. before any checkpoint could be saved), we would restart training. The following hyperparameters were used for the final experiments:

```
hyp = {
    "input_dim": input_size,
    "hidden1_dim": 1024,
    "hidden2_dim": 512,
    "hidden3_dim": 256,
    "zc_dim": 2,
    "emb_dim": 128,
    "n_gmm": 2,
    "dropout": 0.5,
    "lambda1": 0.1,
    "lambda2": 0.005,
    "lr": 1e-4,
    "batch_size": 256,
    "epochs": 1000,
    "patience_epochs": 10,
    "checkpoint": "best",
    "return_logits": False,
}

# Taken from KDDCUP-Rev config from original DAGMM paper
# Most other configs are unstable and frequently result in NaNs during training
if config.data.dataset in ["probe", "u2r"]:
    hyp["hidden1_dim"] = 120
    hyp["hidden2_dim"] = 60
    hyp["hidden3_dim"] = 30
    hyp["emb_dim"] = 10
    hyp["n_gmm"] = 4
    hyp["zc_dim"] = 1
    hyp["batch_size"] = 1024
    hyp["return_logits"] = True
    hyp["lr"] = 1e-5

if config.data.dataset == "bank":
    hyp["hidden1_dim"] = 64
    hyp["hidden2_dim"] = 32
    hyp["hidden3_dim"] = 16
    hyp["emb_dim"] = 10
    # hyp["zc_dim"] = 1
    hyp["batch_size"] = 4096
    hyp["lr"] = 1e-5

if config.data.dataset == "census":
    hyp["hidden1_dim"] = 256
    hyp["hidden2_dim"] = 128
    hyp["hidden3_dim"] = 64
    hyp["emb_dim"] = 10
    hyp["lr"] = 1e-5
```



Figure 3: Samples from Top-K=50 GNSM rankings. The columns (repeated) show input image, ground truth segmentations, and model predictions respectively.

A.3 EXTENDED RESULTS

Below we show the predictions ranked poorly by both DSVDD and our method. Images are displayed in order from highest ranking to lowest (displayed left to right).



Figure 4: Random samples from Top-K=50 DSVD rankings. The columns (repeated) show input image, ground truth segmentations, and model predictions respectively.